

# The SEASAT Synthetic Aperture Radar Experiment

R. C. Beal

*The SEASAT Synthetic Aperture Radar (SAR) has yielded dramatic imagery of our planet from space. It penetrates cloud cover and darkness to reveal subtle changes in landform and a variety of atmospheric interactions with the ocean. This article discusses the concept of aperture synthesis, some peculiar problems of spaceborne SAR, APL's role in the experiment, and examples of the new imagery.*

## Introduction

Many of the meteorological changes that affect our lives from day to day and the continuing climatic changes that occur over the centuries are caused by the vast amounts of energy constantly being transferred back and forth between the atmosphere and the oceans. Global trade winds and an erratic solar flux create large-scale oceanic currents and significant temperature gradients that influence world climate and even control human migration patterns. The Gulf Stream, for example, carries heat from the Caribbean to the seas of Northern Europe, fostering the only large-scale human settlements established closer to a pole than to the equator.

Civilian space programs are increasingly justified on the basis of their applications potential, in particular their ability to demonstrate clear economic or social benefit. Communication satellites have been the most successful in this regard, as measured by the degree of federal subsidy necessary for their survival. On the other hand, navigation and weather satellites have increasing arrays of private users but continue to be funded primarily by the government. Most of them are managed by user agencies and are therefore termed "operational." For a satellite system to become operational is significant because it implies that at least one user agency is sufficiently convinced of its benefit to provide sponsorship. (The Departments of Commerce, Interior, and Agriculture are examples of user agencies; NASA is not.)

We are currently in the midst of an evolutionary period of several decades during which high-resolution images of our planet taken routinely from space are dramatically expanding our environmental sensitivity. Operational weather satellites have been monitoring global cloud movement for several years. The near-operational LANDSAT's are beginning to provide accurate estimates of some global resources, the most notable progress being made in an annual global wheat inventory. During 1978, an experimental microwave-imaging radar was launched as part of SEASAT, the oceanographic satellite (see the Digest, Vol. 16, No. 3), thus opening an entirely new region of the spectrum for monitoring our planet.

In many respects, microwave imagery obtained from orbit complements visible imagery and provides information not otherwise available. Its high resolution is obtained by artificially synthesizing an aperture many kilometers long in space (thus the name synthetic aperture radar, or SAR); as a result, it is both sophisticated and expensive.

SAR has two basic advantages over any other high-resolution sensor: it can collect imagery through cloud cover, without the help of the sun. In addition, it has the proven ability to map details of the polar ice fields and the potential (but not proven) ability to image ocean swell unconditionally. In fact, these are two of the primary reasons for placing the instrument on an oceanographic satellite. The benefits to transoceanic shipping, severe weather prediction, and long range studies

of climatology can be substantial if SAR measures either ice fields or wave fields reliably. Conversely, one of these applications will probably have to be demonstrated conclusively if SAR is to obtain operational status on any future oceanographic satellite.

Having briefly stated some rationale for the experimental SEASAT SAR, this article will discuss the concept of aperture synthesis, the APL hardware involvement, the 98 day lifetime of the SEASAT SAR, the APL ocean-wave detection experiment, an example of the new imagery, and future plans. The subsequent articles will expand on APL's particular contributions to the implementation of the experimental SAR instrument, developed by the Jet Propulsion Laboratory (JPL) of the California Institute of Technology.

## Aperture Synthesis

According to classical diffraction theory, the angular resolution of any transmitting or receiving system, including SAR, is ultimately limited by the size of its aperture. Expressed simply,

$$\phi = 1/n \quad (1)$$

where  $\phi$  is the angular resolution and  $n$  is the size of the aperture, expressed in wavelengths. When the same aperture is used for both the transmitter and the receiver of energy, as it is in SAR, the resulting angular resolution  $\phi'$  is effectively halved ( $\phi' = \phi/2$ ). Now imagine the satellite geometry shown in Fig. 1, typical of the SEASAT SAR parameters, with a satellite orbiting at altitude  $h$  (or slant range  $h$ , for near-nadir geometry) of  $10^6$  m, and containing a SAR that operates at a radar wavelength  $\lambda$  of

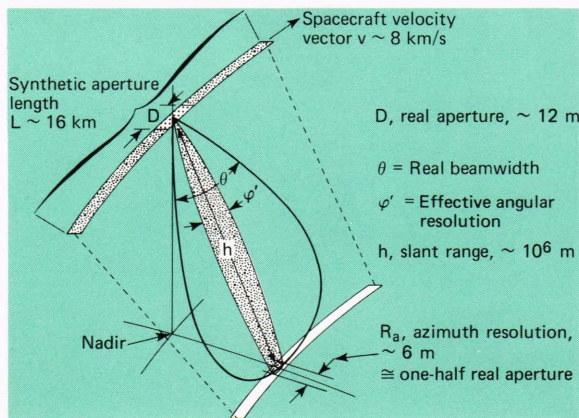


Fig. 1—Ultimate resolution of a synthetic aperture.

0.2 m. The length of the synthetic aperture  $L$  is related to the azimuth resolution (the ground resolution in the flight direction of the spacecraft),  $r_a$ , by

$$r_a = \phi' h = \frac{\lambda}{2L} h. \quad (2)$$

An azimuth resolution of 25 m requires the synthetic aperture to be 4 km long. A satellite traveling at about  $10^6$  m has an orbital velocity of about 8 km/s, and therefore requires about 0.5 s to synthesize the required aperture.

Note that the length of the real aperture  $D$  on the spacecraft has not explicitly entered into the equations. However, the real aperture must be short enough to allow a particular point on the ground to remain entirely within the real beam  $\theta = \lambda/D$  during the aperture synthesis interval. This leads to the relationship (again illustrated in Fig. 1)

$$L = h \frac{\lambda}{D} \quad (3)$$

where  $D$  is the length of the real aperture and  $L$ ,  $h$ , and  $\lambda$  have been defined above. Combining (2) and (3) leads to the fundamental lower limit for resolution<sup>1</sup>

$$r_a = D/2. \quad (4)$$

Therefore, if a ground resolution of 25 m is desired, the real aperture can be no longer than 50 m to maintain a point in the real beam for a long enough time. The resolution limit is independent of range because the time during which a particular point is illuminated increases with range, thus allowing a correspondingly larger synthetic aperture to be formed. The SEASAT SAR had a real aperture length of about 12 m and thus was theoretically capable of an azimuth resolution of 6 m. This assumes that the maximum allowable synthetic aperture of 16 km could be constructed, a distance that is transited by the satellite in about 2 s.

Although a 6 m azimuth resolution from SEASAT is theoretically possible, the imagery is typically processed to yield only 25 m. That is, only 4 km of synthetic aperture (0.5 s of data) is processed at a particular instant of time. Any 4 km from the total 16 km length will satisfactorily produce a resolution of 25 m. Moreover, since the predominant system noise in the SAR is caused by "coher-

<sup>1</sup> L. J. Cutrona, W. E. Vivian, E. N. Leith, and G. O. Hall, "A High Resolution Radar Combat-Surveillance System," *IRE Transactions, MIL-5* (1961).

ent speckle," which tends to be Rayleigh-distributed in amplitude (i.e., there are wide variations in the reflected signal from a resolution element as the illumination angle is slightly varied), each 4 km segment potentially allows an independent sample of the "average" reflectivity distribution. Therefore, the variance within a scene can be reduced considerably by separately processing and combining four independent 25 m images.

So far our discussion has dealt only with the very basic criteria for obtaining high azimuth resolution along the velocity vector of the satellite. We have not examined the actual mechanics of collecting and processing the information to reform the image, nor have we expanded our discussion to include the orthogonal (range) dimension. It should be apparent, however, that the synthetic aperture must be constructed with extreme care to realize fully its potential. For example, the resolution suffers if the satellite is perturbed from the perfect trajectory by a significant fraction of its operating wavelength (about 5 cm) as it traces out the 16 km aperture. This is equivalent to forming an image in a camera with a scratched or distorted lens. Various types of aberrations can occur, all of which lead ultimately to loss of resolution and contrast in the image.

Having explored some of the fundamental requirements for aperture synthesis, Fig. 2 summarizes schematically the major steps in forming an image in terms of a point source response. Because an imaging system must be linear to first order, superposition arguments can extend the result

to an arbitrary distribution of radar backscatter. A point source (step 1), having been illuminated by a coherent radar, emits a series of concentric wavefronts (step 2). Of course, the emission occurs only while the point source is within the aperture beam, as was discussed above. The spacecraft cuts through the concentric wavefronts (step 3), and the SAR receiver intercepts an energy flux that varies with position (or time) as the wavefronts are traversed (step 4). This wavefront record has several names: it is the doppler or phase history to radar engineers, and it is the hologram, diffraction pattern, or one-dimensional zone plate to those with an interest in optics. The essential point is that this wavefront record, which contains a complete phase and amplitude history of the point source for the entire synthetic aperture interval, is all that is required to reproduce a diffraction-limited version of the original point source. The wavefront record is transferred from the spacecraft to any of several ground stations through a data link (step 5), where it is recorded, usually on digital tape or optical film. For SEASAT, the record was normally recorded on tape at the station and later transferred to film at a central facility. To reproduce the point source from the wavefront record, a coherent reference function (step 6) (such as a family of plane waves from a laser) impinges on the phase history (step 7). The phase history, which is essentially the diffraction pattern of a point source, causes a lensless convergence of the plane waves in free space (step 8) to form a replica of the original point

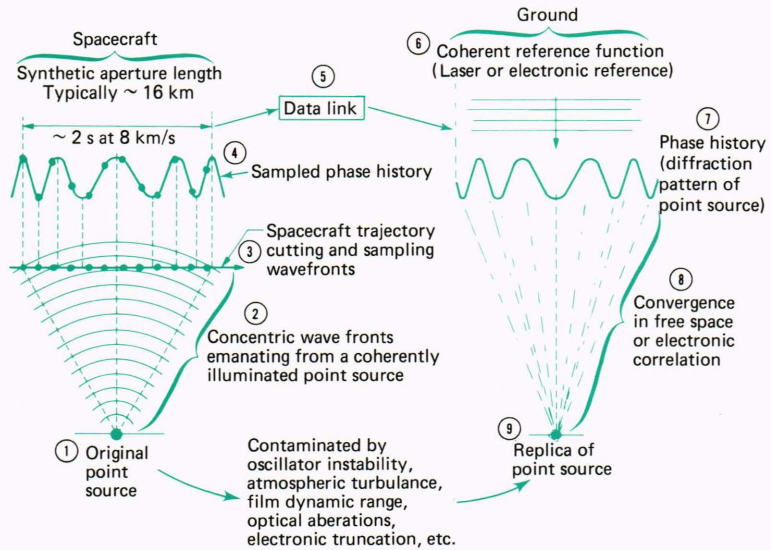


**Fig. 2—Construction of a synthetic aperture.**

source, thus completing the cycle.

In practice, there are several variations to the simple scheme described in Fig. 2, some of which are helpful, some nuisances, and others destructive. A simple lens inserted at step 8 shortens the convergence distance and thus is helpful. On the other hand, the spacecraft trajectory (step 3) is better described by an arc of varying center of curvature than by a straight line. Thus, the diffraction pattern becomes a function of time, which is clearly a nuisance entailing an adaptive processing strategy. Atmospheric turbulence, reference function instabilities, and lens aberrations are examples of destructive and basically uncorrectable sources of contamination. Much of the effort and expense of the SEASAT SAR can be directly attributed to the need to account for the systemic sources of contamination and to minimize the random sources.

The extension of SAR image formation to the range (cross-velocity) direction is straightforward, but it places strict timing and synchronization requirements on the design and severely restricts the total range interval (or corresponding ground swath width) that can be accommodated. Range information is possible in a SAR only because the synthetic aperture need not be continuous but may be constructed with samples; that is, the transmitter may be pulsed. It is enough that one pulse be transmitted each time the real aperture moves by half its length. This is called "filling the aperture" and leads to a maximum time interval  $\tau$  of  $D/2v$  during which range information can be collected. For a  $D$  of 12 m and a  $v$  of 8 km/s,  $\tau$  equals 750  $\mu$ s. In actual practice, the aperture is slightly "overfilled" to reduce the possibility of spurious signals that could reduce contrast. The SEASAT SAR, for example, typically operates at an interpulse period of 600  $\mu$ s. Moreover, somewhat less than half of this time interval represents signals of sufficient quality to produce good imagery.

Figure 3 shows the synchronization constraints imposed by the SEASAT geometry. Transmitter pulses are emitted every 600  $\mu$ s in the cross-track direction, 20° away from nadir. They form concentric expanding rings of energy with a separation of about 200 km ( $c\tau = 3 \times 10^8 \text{ m/s} \times 600 \times 10^{-6} \text{ s} \approx 200 \text{ km}$ ). With the satellite orbiting at an altitude of 800 km, there are four such pulses descending at any time. Since the antenna illuminates only that region around 20° from nadir, no significant backscatter occurs except at a slant range of about

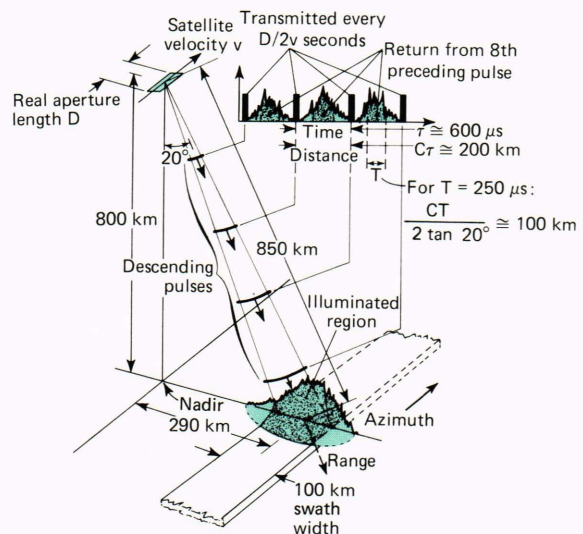


**Fig. 3—Synchronization constraints in the SEASAT SAR.**

850 km. This is no accident, since the round trip distance of 1700 km must be chosen to allow the return from a particular pulse to occur exactly between two subsequently transmitted pulses. The geometry and pulse interval for the SEASAT SAR are chosen to allow the return from a given pulse to occur exactly midway between the eighth and ninth subsequent pulses. As Fig. 3 shows, the middle 250  $\mu$ s of return represents a swath width of about 100 km for the SEASAT geometry. It is particularly significant that large swaths inherently require very long real apertures, thus increasing the time needed to collect information from large range differences, while still allowing the synthetic aperture to be filled properly. This is one of the more serious limitations in spaceborne SAR's.

## The APL Involvement

The candidate SAR for SEASAT posed a curious dilemma in 1974. User surveys conducted by APL (then performing a mission study for NASA) indicated that the most useful operational output from the SAR would be a matrix of global ocean wave spectra (i.e., the direction and wavelength of the predominant swell components) every few tens of kilometers, but over a swath of several hundred kilometers.<sup>2</sup> Such a global matrix would present a trivial data transmission problem involving fewer than 100 bits/s and could dramatically improve

<sup>2</sup> *SEASAT-A Definition Phase Baseline Mission Report*, APL/JHU SDO 3831 (1974).

existing wave forecast models. This strategy, although conceptually attractive, proved impractical to implement for the following reasons:

1. The scattering physics by which SAR images ocean waves was not, and still is not, well understood. In particular, the bounds of surface winds, ocean swell, and radar geometry and wavelength over which wave detection is possible had not been thoroughly and systematically studied.
2. To produce a complete two-dimensional wave spectrum, assuming the swell was detectable, all the steps of Fig. 2 would have to be duplicated on the satellite and in real time. This might involve a two-dimensional cross correlation, several thousand elements on a side, with time-varying reference functions. Such parallel adaptive processing in small spaces is still beyond the state of the art.
3. A swath several hundred kilometers wide requires a real aperture several tens of meters long which, although perhaps feasible, would be difficult and expensive.

An additional and perhaps even more fundamental objection to the idea of bandwidth reduction is that the image is forever lost. Much of the excitement of SAR in space is that it can deliver a new kind of image with a scientific potential that is difficult to anticipate. Therefore the very idea of spacecraft preprocessing for data rate reduction is not acceptable to a large portion of the user community. At this early stage, when applications are being actively explored, the full and uncontaminated radar backscatter map may be the most useful data product.

For these kinds of reasons, the SEASAT SAR was configured to yield raw unprocessed phase and amplitude signals, without any attempt to prejudge the inherent information content of the imagery. APL examined various data-link configurations to allow a maximum information flow at minimum cost. A number of digital, analog, and hybrid options were considered and, in June of 1974, a direct analog transmission with PRN (pseudorandom noise) encoding was recommended to NASA<sup>3</sup> for the following reasons:

1. All the information from a 100-km-wide

swath at 25 m resolution would be preserved with less than 20 MHz bandwidth.

2. LANDSAT compatibility could be ensured by using an existing 20 MHz channel allocation and portions of receiver hardware that was already installed in several domestic and foreign ground stations.
3. A significant amount of hardware required for high-speed digitization and formatting could be transferred from the spacecraft to the ground.

The essential APL task was to design and implement a data system that not only removed the one-way doppler effect of the satellite but also kept satellite timing information to within a small fraction of a range resolution element. Fortunately, recent work at APL on the Transit Improvement Program had conclusively demonstrated techniques that permitted timing recovery to a few nanoseconds in the presence of satellite doppler. The elegant combination of doppler and range tracking that resulted in an essentially contamination-free link is described in a companion article.

Several months after the data-link effort began, APL was asked to create the system for providing high-density digital tapes from the analog return. This task primarily involved high speed (240 Mb/s) digital-to-analog conversion, buffering, and formatting of the data, although some sophisticated SAR simulation equipment was also developed. Some of this simulation equipment later proved invaluable for an accurate assessment of total system performance just prior to launch. The APL effort in these areas is described in the last article of this issue.

## The 98-Day SAR Experiment

On July 4, 1978, approximately one week after SEASAT was launched, SAR was successfully operated over the Goldstone tracking station. On October 10, as it was passing over the horizon of the United Kingdom station at Oakhanger, the entire satellite died prematurely because of a power system failure. In the 98 days during which SAR was operating, nearly 500 high-density digital tapes were collected at three domestic and two foreign stations. One year later, less than one-third of the tapes had been converted to imagery. However, it is already clear that the tapes contain a wealth of imagery that will take several years to analyze and assess fully.

<sup>3</sup>R. C. Beal, "SEASAT Imaging Radar Data Transmission: The Case for an Analog Downlink," APL Internal Memorandum S3R-75-093, 27 June 1975.

Because of the relative uncertainty of the ultimate application for spaceborne SAR (i.e., that application for which some user agency is willing to pay), the validation experiments vary widely in content. They all have one thing in common, however. A proper validation experiment, of which there are approximately 30 with the SEASAT SAR, must be a comparison between SAR and some more direct (or in situ) measurement of a common quantity. Typical physical parameters of interest in the SAR experiments are ocean wavelength and direction, ice age and thickness, soil moisture content, and geological surface roughness.

A properly conducted validation experiment requires not only extensive preparation but a knowledge of where the satellite will be on a particular date. Unlike the other sensors, the SEASAT SAR caused a considerable drain on the satellite power system and was therefore limited to only one hour of pre-programmed operation per day. In fact, during the first two weeks of September 1978, spacecraft problems limited total SAR operation to only 10 minutes per day.

Throughout the life of the experiment, it was a challenge for an individual investigator to know when the SAR would be over his particular site and to ensure that it would be activated at the proper time. Fortunately, close cooperation between the investigators and the JPL project personnel made

possible what could easily have been impossible. In one extreme case, an entire team that was conducting a soil moisture experiment was transferred overnight with its instrumentation from one state to another.

Figure 4 is a sequence of the SAR coverage for each week of its lifetime. The five circles are the 10° elevation masks for each of the three domestic and two foreign stations. The largest number of passes were recorded at Goldstone, but nearly as many were recorded at Fairbanks and at Merritt Island.

Because of a lag in international agreement, the two foreign stations initially were not equipped to receive data. The European station began recording during the sixth week, the Canadian during the ninth. Just as the Canadians were beginning to record data routinely, the spacecraft developed a thermal problem, and SAR operation was significantly curtailed during the tenth through twelfth weeks. However, in the tenth week, the satellite was placed in a "three-day-repeat" orbit to facilitate altimeter calibration over Bermuda. This repeating orbit caused the satellite to pass over exactly the same subpoints at three-day-plus-12-minute intervals and greatly facilitated the planning of validation experiments. By the thirteenth week (the middle of September), the 10-minute-per-day operating limit had been lifted, the orbit was well

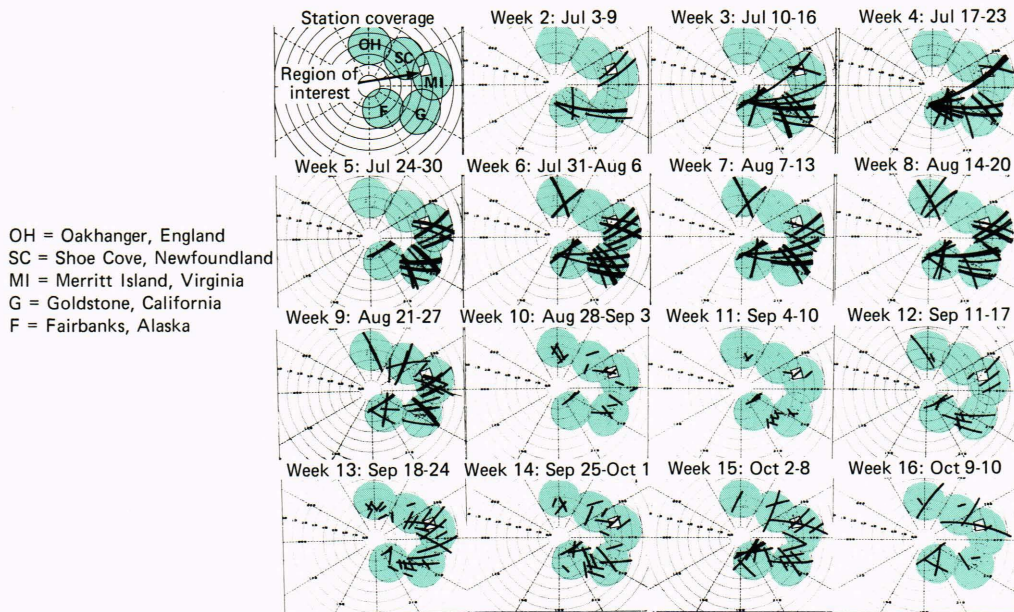


**Fig. 4—Weekly history of SAR coverage for each of the five stations (Polar view).**

defined and repeating, and all five stations were receiving comparable quantities of data.

This optimal situation continued for slightly more than three weeks, until the satellite's demise at the beginning of the sixteenth week. By then, the altimeter had been fully calibrated, and the satellite was scheduled momentarily to be placed into a "baseline" orbit that would have allowed the instrument subtracks to progress slowly to the east at a rate of approximately 10 km every three days.

In spite of the early extinction of the satellite and the various planning obstacles cited above, a surprising number of validation experiments were successfully carried out, beginning around the middle of August. One of the more comprehensive experiments was organized by NOAA in the Gulf of Alaska under the acronym GOASEX (for Gulf of Alaska SEASAT Experiment). GOASEX involved several government organizations and universities and was specifically designed to collect the necessary "surface truth" to assist in validating the wind and wave measurement capabilities of each of the spacecraft's sensors. Two GOASEX workshops were held in 1979, and significant results for each of the instruments are beginning to appear in the literature.<sup>4</sup> Several other experiments, including a joint U.S./Canadian ice dynamics study, are currently in various stages of analysis.

## SAR Ocean Wave Detection and "Duck-X"

The spatial distribution of microwave backscatter in a SAR image is a function of at least the roughness of the surface and its dielectric constant. The strength of the return depends on a "Bragg resonance" at the operating wavelength of the sensor, which is typically in the region of 3 to 30 cm. A high density of Bragg scatterers in this region can be described as "rough" at the radar wavelength, tending to diffuse the incident energy in all directions (including the incident direction). A smooth surface tends to be specular, however, acting as a mirror. Unless the incident direction is normal to the surface (as it is in the altimeter), very little energy from smooth surfaces is reflected back toward the transmitter. As a particular example, SAR cannot form images of ocean swell unless there is a consistent variation of Bragg scat-

terers from the peaks to the troughs of the swell.

There are a number of physical mechanisms that could produce this modulation of the scatterers, none of which predominates under all conditions. It is even possible that, for some surface wind conditions and viewing geometries, the scattering modulation does not exist, causing the swell to "disappear" in the SAR image. On the other hand, it is conceivable that a correct choice of wavelength and geometry for future SAR's might allow successful imaging of ocean swell for almost any surface wind condition. To study this problem properly, one would like to understand how the two-dimensional energy distribution behaves in the 3 to 30 cm region of the ocean. Although significant progress has been made on this subject recently, much remains to be discovered.

Consider the hypothetical spectrum (a Fourier transform of the elevation of the sea surface) shown in Fig. 5, composed of both "sea" and "swell." The swell components, which are the only portions of the spectrum capable of being imaged by SAR, are the result of spatially and temporally remote wind fields. That is, they are entirely independent of the concomitant wind field. Conversely, at the other end of the spectrum, for waves of order 3 cm, the form of the spectrum is more tightly coupled to the instantaneous, high-frequency components of the wind. For turbulent, gusty winds that often occur at the boundary layer, the short-wave spectrum might be nearly isotropic directionally. The longer, small gravity waves (30 cm) take somewhat longer to generate and can be expected to be more aligned with the average direction of the wind.

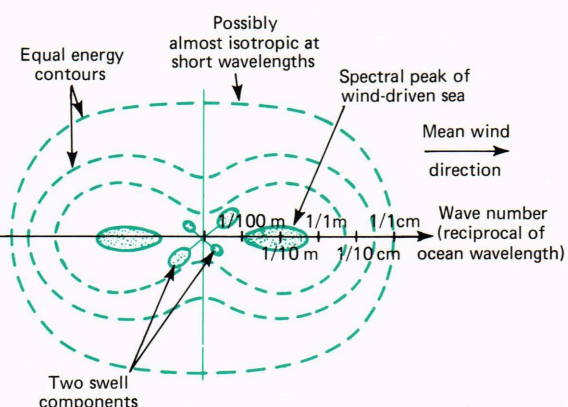


**Fig. 5—Possible form of the two-dimensional ocean elevation spectrum over five decades in wave number.**

<sup>4</sup> Preliminary results from each of the SEASAT sensors are described in a series of articles in *Science* 204 No. 4400 (1979).

The presence of swell is known to influence the energy in the short-wave portion in the form of a modulation. The modulation is essential if SAR is to image the swell. Ideally, one would choose an interaction wavelength for SAR such that the modulation is both maximized and isotropic in azimuth. Furthermore, if the modulation depth could be described as a known function of wind speed and some wave parameter (either height or slope), a SAR could be designed not only to detect the wavelengths and direction of swell, but also to obtain a measure of its energy. It will be surprising if nature is so accommodating in all of these ways. On the other hand, a more complete knowledge of the behavior of the spectrum would allow an optimization not presently possible.

The Duck, North Carolina Experiment (Duck-X) was one of three major SEASAT SAR wave-detection experiments conducted with extensive coincident surface truth during the limited lifetime of the SAR. APL and a number of government agencies cooperated in a series of microwave, optical, and in-situ measurements of the ocean, generally coincident with the SEASAT overflights. Fortunately, the Duck site was located almost directly beneath the three-day repeat orbit that existed from August 28 to October 10, 1978. During that time 14 ascending daylight passes came over or within 15 km to the east of Duck. An additional corresponding set of descending nighttime passes came within 70 km to the east of Duck. Of 30 passes for which SAR imagery was requested, 23 were recorded and now exist on tape.

The Duck-X data set, by a mixture of good fortune and good planning, is one of the most comprehensive imagery sets collected during the SEASAT lifetime. A particularly rich sequence of 14 ascending passes at three-day intervals starting on August 29 and continuing until October 7 (only three of which are missing) covers a large portion of the Atlantic off Cape Hatteras, extends up the Chesapeake Bay, and eventually crosses the Appalachians. Only four of this set have been processed to imagery at present, but they have shown several remarkable features. For example, ocean waves of significant height ( $0.65 \text{ m} \pm 0.25 \text{ m}$ ) and length (200 m), that are present on September 28, correlate well with simultaneous aircraft radar, laser, and in-situ measurements.

As the imagery from SEASAT undergoes more extensive and intensive analysis, the present and future potential of SAR in space will become in-

creasingly clear. The new imagery will stimulate much debate about the usefulness of SAR for both scientific and reconnaissance purposes. Potential user agencies will each assess SAR according to their own needs and resources. The debate has been going on for some time and can be expected to become livelier with the new imagery.

## An Example of the New Imagery

Just after 11 a.m. EDT on September 25, 1978, the SEASAT SAR was activated for a five minute pass off Cape Hatteras in support of Duck-X. One of the bonuses of this pass and of several others in the Duck-X data set is the complete image of the Chesapeake Bay region of eastern Maryland shown on the cover. A two-fold enlargement of the northwest portion of the cover image, shown in Fig. 6a, encompasses an area from western Howard County past Baltimore harbor on the north and from lower Prince Georges County past Tilghman Island on the south. The figure gives some indication of the ultimate resolution limits of SAR and how its characteristics differ from more conventional, visible satellite photography.

Note first that clouds are completely transparent to the radar. Bright return suggests either a rough, diffuse scatterer (at 30 cm) or a local slope oriented normal to the satellite (i.e.,  $20^\circ$  from horizontal). Clusters of man-made objects, such as cities, tend to have many metallic and smooth corner reflectors and produce bright return. Dark return suggests smooth (untilted) and highly reflective surfaces, or absorptive ones. Wet marshes, wind-sheltered rivers and bays, airport runways, and highways are consistently dark. Cleared land with cover less than 30 cm high tends to be dark. Dry flood plains (presumably with cover greater than 30 cm) tend to be diffuse and bright. Some of the more obvious features of Fig. 6a are described below. The discussion is keyed to the numerical callouts on Fig. 6b.

The middle Chesapeake Bay region (1) below the Bay Bridge (2) is relatively bright, indicating that wind-induced waves are present. Near-shore regions of the Bay (3) on the leeward side of the land are dark, indicating smooth, sheltered water surfaces. A cluster of five ocean vessels (4) (probably tankers) is located just below the Bay Bridge. No wakes are visible, although they are often observed in the imagery. The western entrance of the Bay Bridge (2) is brighter and more well defined

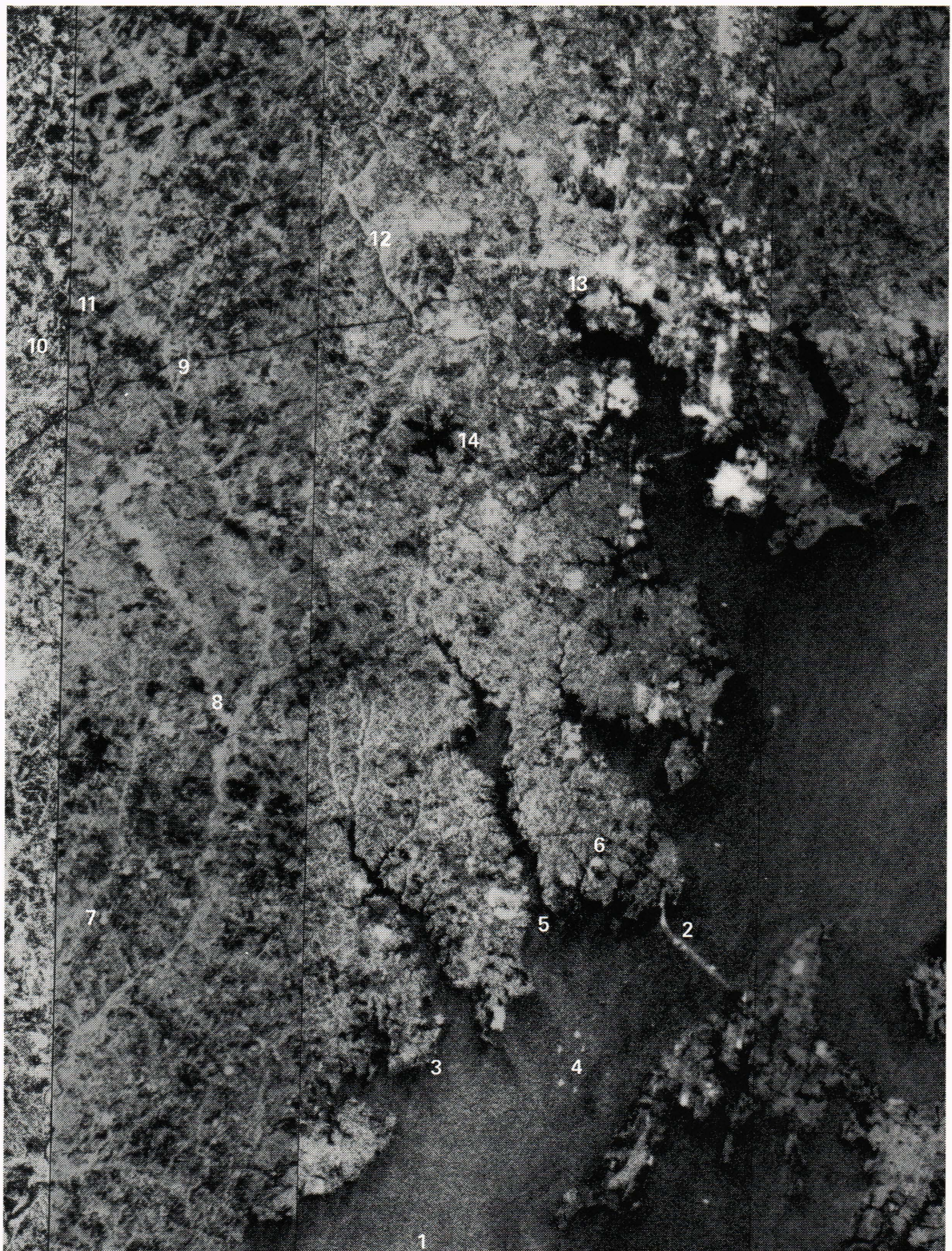
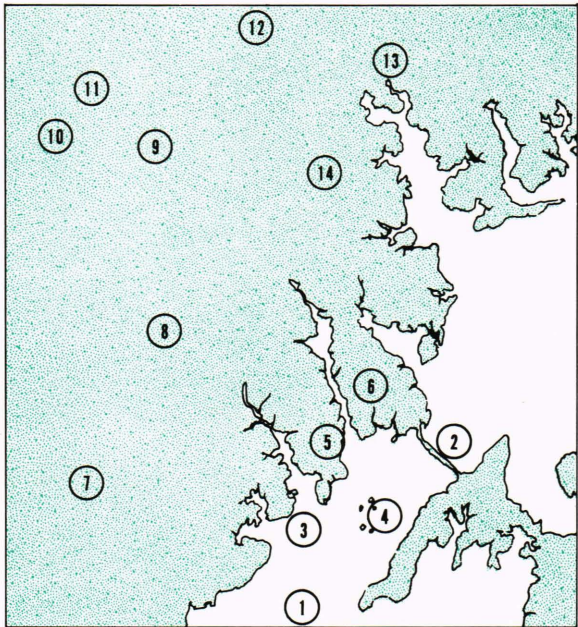


Fig. 6a—An enlargement of the cover image's northwest portion. It encompasses an area from western Howard County to Baltimore harbor on the north and from lower Prince Georges County to Tilghman Island on the south.



**Fig. 6b—Callouts corresponding to features visible in Fig. 6a**

than the rest because it is nearly parallel to the spacecraft velocity vector. Annapolis (5) is also bright, but U.S. Route 50 leading to the bridge (6) is dark.

The Patuxent River (7) can be seen clearly to converge from three streams, and the easternmost branch can be followed through several more smaller convergences (8), well past Interstate 95 (9). This ability of the SAR to follow riverbeds may be peculiar to radar and certainly exceeds that of LANDSAT. Rocky Gorge Reservoir (10) is clearly outlined, but the APL complex (11) is not apparent. The fall line (the boundary between piedmont and coastal plain) runs just north of Interstate 95, so there are few extensive steep slopes ( $>20^\circ$  for a distance of 25 m) in the figure. A notable exception, however, is the Patapsco River Basin (12), which has cut a deep gorge nearly to the Bay. The gorge is characterized by an adjacent band of light and dark in the direction parallel to the satellite path. The bright return represents terrain on the far slope, normal to the incident energy. The dark return represents near-slope return that is shadowed from the satellite (i.e., greater than  $20^\circ$  slope). Baltimore City (13) is generally bright, with some of the downtown street pattern vaguely suggested. The runways at Baltimore-Washington International Airport (14) are dark.

## The Future

Figure 6a may appear somewhat grainy to the reader compared to similar visible images taken from space, such as from LANDSAT. The SAR image is noisier and of lower contrast, even though the inherent resolution is three times better than that of LANDSAT (25 m versus 80 m). The simplest explanation is that SAR is energy starved. For example, Fig. 6a was created by illuminating about 3000 km<sup>2</sup> of Maryland with 25 W of microwave power for less than 10 s. Very little energy is spent interrogating a particular resolution element to determine its average reflectivity. Consequently, there is much uncertainty in the response.

Without suffering a loss either of resolution or of swath width, the uncertainty can be reduced only with (a) a more powerful radar that consumes perhaps 1 to 10 kW of spacecraft power, (b) a longer antenna (up to 50 m), or (c) a lower altitude. The first two options are possible but expensive. The third is the most obvious and has the advantage of entailing no risk. The next orbiting SAR, in fact, will use the Shuttle capability to conduct a several-day-long experiment at an altitude of 200 km. Unfortunately, the experiment will be short and the orbit will be confined to lower latitudes. Therefore, ice and ocean dynamic studies will not be possible; the main emphasis is expected to be on land applications.

Beyond the early Shuttle mission, several U.S. government and foreign agencies have active studies that may eventually lead to the next earth-orbiting SAR. The next U.S. mission to Venus will probably include a SAR. Any future international ice dynamics satellite might also include a SAR. There is an extensive body of literature that describes the all-weather capability of SAR for mapping crops and soil moisture as an adjunct to the LANDSAT imagery. A European consortium, anxious about the nonoperational status of LANDSAT, is studying a spacecraft that would collect both high-resolution visible and microwave imagery.

It has been nearly 30 years since the first practical demonstration of SAR, 15 years since it was proposed for an oceanographic satellite, and little more than one year since the first SAR was placed in orbit. The continuing evaluation of the SEASAT imagery will help greatly in the natural evolutionary process of defining the future of SAR in space.